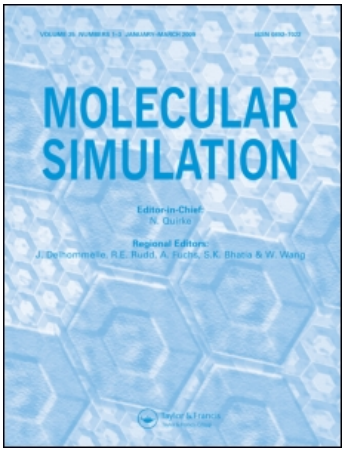

Molecular Simulation
Publication details, including instructions for authors and subscription information:
http://www.informaworld.com/smpp/title~content=t713644482

Molecular dynamics simulation of energetic uranium recoil damage in zircon

R. Devanathan[a]; L. R. Corrales[a]; W. J. Weber[a]; A. Chartier[b]; C. Meis[b]
[a] Fundamental Science Directorate, Pacific Northwest National Laboratory, Richland, WA, USA [b] CEA Centre d'Etudes de Saclay, Gif-Sur-Yvette, France

To cite this Article Devanathan, R. , Corrales, L. R. , Weber, W. J. , Chartier, A. and Meis, C.(2006) 'Molecular dynamics simulation of energetic uranium recoil damage in zircon', Molecular Simulation, 32: 12, 1069 — 1077
To link to this Article: DOI: 10.1080/08927020600959929
URL: http://dx.doi.org/10.1080/08927020600959929

Molecular Simulation, Vol. 32, Nos. 12–13, 15 October–15 November 2006, 1069–1077

Taylor & Francis
Taylor & Francis Group

Molecular dynamics simulation of energetic uranium recoil damage in zircon

R. DEVANATHAN†*, L. R. CORRALES†, W. J. WEBER†, A. CHARTIER‡ and C. MEIS‡

†Fundamental Science Directorate, Pacific Northwest National Laboratory, Richland, WA 99352, USA
‡CEA Centre d'Etudes de Saclay, 91191 Gif-Sur-Yvette, France

(Received July 2006; in final form July 2006)

Defect production and amorphisation due to energetic uranium recoils in zircon ($ZrSiO_4$), which is a promising ceramic nuclear waste form, is studied using molecular dynamics (MD) simulations with a partial charge model. An algorithm that distinguishes between undamaged crystal, crystalline defects and amorphous regions is used to develop a fundamental understanding of the primary damage state. The amorphous cascade core is separated from the surrounding crystal by a defect-rich region. Small, chemically inhomogeneous amorphous clusters are also produced around the core. The amorphous regions consist of under-coordinated Zr and polymerised Si leading to amorphisation and phase separation on a nanometer scale into Zr- and Si-rich regions. This separation could play an important role in the experimentally observed formation of nanoscale ZrO_2 in $ZrSiO_4$ irradiated at elevated temperatures.

Keywords: Molecular dynamics; Amorphisation; Nuclear waste form; Uranium recoil

1. Introduction

The immobilisation of high level nuclear waste and excess weapons plutonium in a suitable ceramic host material is an urgent concern from the standpoint of environmental protection, national security and non-proliferation. Due to the anticipated expanded use of nuclear energy to meet growing global energy demand, there is a pressing need to design nuclear waste form materials based on a fundamental understanding of radiation effects in ceramics. Atomistic computer simulation is needed to develop such an understanding; because the small time (ps) and distance (nm) scales of primary radiation damage production in materials preclude direct experimental observation. At the same time, energetic radiation damage processes cannot be simulated by accurate *ab initio* calculations due to computational limitations. Thus, classical molecular dynamics (MD) simulation using reliable empirical potentials is ideally suited to the task at hand.

This report presents the findings of a classical MD simulation of the primary damage state produced in zircon by 10 and 30 keV U recoils. Zircon is a promising ceramic host material for actinide immobilisation, because it is a durable mineral that occurs in nature with up to 5000 ppm $UO_2 + ThO_2$, but has been known to occur with total U and Th concentrations up to 7 wt% [1]. Moreover zircon has been synthesised with 10 wt% Pu loading [2]. α-decay events in actinide-bearing $ZrSiO_4$ result in a 4–6 MeV α particle that loses its energy by ionisation and isolated defect creation and a 70–100 keV recoil that creates a cascade of atomic displacements leading to amorphisation. It is unclear whether amorphisation proceeds only by direct impact in the cascade or by a combination of direct impact and accumulation of defects formed around the cascade core. Experimental evidence can be found in support of both these models [1]. MD simulation has been used previously to model radiation damage in zircon [3,4]. Crocombette and Ghaleb [3] observed Si atoms with the unusual coordination of five oxygen neighbours and Zr atoms with 6.5 neighbours on average following 4 and 5 keV U recoils and concluded that an amorphous core forms in the cascade in zircon. They quantified the extent of the disorder based on the first neighbour environment of the cations and the degree of Si—O—Si polymerisation [3]. Trachenko *et al.* [4] have also observed such polymerisation and local density changes in their study of 30 and 70 keV Zr cascades in $ZrSiO_4$. However, the

*Corresponding author. Tel.: + 1-509-376-7107. Fax: + 1-509-376-5106. Mailstope: K8-93. Email: ram.devanathan@pnl.gov

Molecular Simulation
ISSN 0892-7022 print/ISSN 1029-0435 online © 2006 Taylor & Francis
http://www.tandf.co.uk/journals
DOI: 10.1080/08927020600959929

number and types of defects produced were not analysed in detail. Our previous work with 0.25–5 keV recoils of U, Zr, Si and O in zircon revealed the occurrence of Si—O—Si polymerisation even for low energy (0.25 keV) recoils [5].

In the present work, MD simulations of 10 and 30 keV U recoils in $ZrSiO_4$ have been performed with a partial charge model. The main objective of the present work is to understand the primary damage state produced by U recoils in zircon and the atomistic mechanisms responsible for the amorphisation and volume swelling in irradiated zircon. The primary damage state has been analysed in detail using a newly developed criterion for identifying crystalline defects and amorphous regions. In the following sections, the computational methodology is presented and results are discussed in light of experimental observations.

2. Details of the simulation

MD simulations of U recoils in $ZrSiO_4$ were performed using the DLPOLY3 computer code [6]. The interaction between the ions was modelled using a partial charge model [7] developed at CEA Saclay. Since the details of the U—O interaction were not published in the previous work [7], we present the details of the potential here. The model consisted of a Coulombic interaction given by

$$V_{ij}^{C} = \frac{q_i q_j e^2}{4\pi\varepsilon_0 r_{ij}} \tag{1}$$

where q_i and q_j are the charges of the ions interacting at a distance r_{ij}, e is the electron charge and ε_0 is the vacuum permittivity, and a Born–Mayer interaction at distances less than 10 Å for Zr—O, U—O, Si—O and O—O pairs given by

$$V_{ij}^{B} = A_{ij}\exp\left(-\frac{r_{ij}}{\rho_{ij}}\right). \tag{2}$$

The parameters A_{ij} and ρ_{ij} for the Zr—O, Si—O and O—O interactions and the charges q for the Coulomb potential for Zr, Si and O have been reported previously [7]. The charge of U was $+3.8e$. A_{ij} and ρ_{ij} for the U—O interaction, determined by fitting to the structure of coffinite (USiO4), were 5424.8 eV and 0.281723 Å, respectively. This potential was smoothly connected to the repulsive Ziegler–Biersack–Littmark (ZBL) potential [8] at distances much shorter than the equilibrium separation using a Fermi function to correctly model energy loss in the cascade. The details of the fit and the ability of our model to reproduce experimentally determined equilibrium properties have been discussed previously [7]. The Fermi function parameters for the U—O interaction were the same as those reported previously for the Zr—O interactions [7]. The Born–Mayer interaction potential was not used for cation–cation interactions. These interactions were governed by the Coulomb potential.

The simulation cell was initially equilibrated at a constant temperature of 30 or 300 K and zero external pressure for 3 ps in the NPT ensemble. The microcanonical ensemble was used for the cascade simulations. The Coulomb term was calculated using smooth particle mesh Ewald technique and the velocity Verlet algorithm was used to integrate the equations of motion [6]. A certain kinetic energy was imparted to a U atom with initial velocity along a specific crystallographic direction and the evolution of the system was followed for about 15 ps. This initial U recoil was started from a substitutional site on the Zr sublattice within the simulation cell.

For 10 keV U recoils, the initial temperature was 30 K and the box size was about 132 × 132 × 134 Å (20 × 20 × 22 unit cells = 211,200 atoms). Three cases were simulated with initial velocities along [5 5 6], [1 1 8] and [8 1 8] directions. High index directions were chosen to avoid channeling of the recoil. In this case, the temperature of the cell rose from 30 K to a maximum of about 395 K, but settled to a final temperature of about 200 K after 0.2 ps. For comparison, a 30 keV U recoil along [5 5 6] was simulated at 30 K using a box size ~198 × 198 × 201 Å (30 × 30 × 33 unit cells = 712,800 atoms). The temperature rose from 30 K to a maximum of about 350 K and reached a near constant value of 185 K after 0.2 ps. Additionally, to examine the effect of temperature, a 30 keV U recoil was simulated at 300 K along [1 1 8] with a slightly larger box size of ~232 × 232 × 232 Å (35 × 35 × 38 unit cells = 1,117,200 atoms). The temperature rose from 300 K to a maximum of about 500 K and reached a constant value of about 400 K within 0.2 ps. Energy conservation was excellent and fluctuations in energy were smaller than 1 in 10^6 due to the use of a dynamic variable time step algorithm [6] with a minimum time step of 0.01 fs and a maximum of 1 fs.

There are several criteria for the identification of defects in simulated cascades. An atom can be considered a defect if it is displaced more than a certain distance, typically 2 Å. However, it is quite possible for the displaced atom to occupy a perfect lattice site at the end of the displacement as in the case of replacement collision sequences. This will result in an overestimation of defects. It is also possible for several atoms adjacent to each other to be displaced less than 2 Å each and form an amorphous cluster. In this case, an underestimation of defects will result. Criteria based on occupation of Voronoi polyhedra or Wigner cells centered on ideal lattice sites are suitable only for a low concentration of isolated defects. Analysis of our previous work [5] shows that the application of Wigner cell analysis to high energy cascades fails to reveal the existence of amorphous regions and simplistically identifies defects as vacancies, interstitials and anti-site defects. Thus, the Wigner cell criterion cannot be applied to highly damaged or amorphous regions that are created in collision cascades in zircon [3,4]. Topological rules based on connectivity of structural units such as cation coordination polyhedra can be constructed to distinguish between perfect crystalline

and amorphous regions [9]. The construction of rules for reliable topological analysis in complex multicomponent ceramics such as zircon is not straightforward.

The present work identifies defective and amorphous regions based on insights from previous simulations of amorphous zircon produced by quenching from the melt [7]. It is known that amorphous zircon is characterised by polymerisation of Si units and reduced Zr coordination number (CN) [7,10]. In this study, criteria based on Si and Zr coordination were developed using cut-off distances of 2 and 3 Å for Si—O and Zr—O bonds, respectively, based on radial distribution functions for crystalline and amorphous $ZrSiO_4$ [7]. A Zr atom is a defect if it has a CN less than eight. An O atom is considered a defect if the number of Si atoms within 2 Å is different from the value of one corresponding to crystalline zircon. If this number is more than one, the O defect is a bridge between Si atoms, while a number of zero corresponds to a non-bridging O defect. A Si atom is considered a defect if it is connected to another Si atom via an O bridge. To identify amorphous regions neighbours within 3 Å of the defects discussed above were considered. A defect is considered an amorphous atom if more than half of its neighbours are also defects. By this criterion, the set of amorphous atoms is a subset of the set of defects. The region within the 3 Å radius typically contains about 10 atoms, which means that an amorphous atom is a defect surrounded by at least six other defects.

3. Results and discussion

Figure 1 shows the displacement of three 10 keV U primary knock-on atoms (PKAs) from the starting point on the Zr sublattice. The cascades were initiated from different positions for these three cases. A logarithmic time scale is employed to show the changes over three orders of magnitude from 10 fs to 10 ps. The PKA comes to its resting position within 1 ps after displacements of 71, 61 and 74 Å, respectively, for initial velocity along [5 5 6], [1 1 8] and [8 1 8] directions. For the corresponding 30 keV cascade along [5 5 6] at the same temperature of 30 K, the PKA displacement was 108 Å and the PKA attained it within 1 ps. Despite the differences in crystallographic direction, the displacements of the three 10 keV PKAs nearly fall on the same line up to 0.2 ps, which indicates that the ballistic phase is very similar regardless of PKA direction.

A similar conclusion can be reached from figure 2, which shows the number of energetic atoms with kinetic energy in excess of 1 eV as a function of time for the three 10 keV U PKAs discussed above. Data for U PKAs along [5 5 6], [1 1 8] and [8 1 8] crystallographic directions are indicated by circles, squares and triangles, respectively. The data seems to follow the same curve up to 10 ps. From 0.02 to 0.15 ps, the number of energetic atoms rises sharply as the U recoil transfers its energy to lattice atoms. Subsequently, these atoms lose their energy through heat transfer and defect creation. After about 5 ps, none of the atoms has kinetic energy in excess of 1 eV. From the temperature rise of the simulation cell, it was estimated that half of the initial energy was expended in creating defects and the remaining half was dissipated as heat. The number of amorphous atoms is also plotted in figure 2 as solid, dashed and dash-dotted lines for [5 5 6], [1 1 8] and [8 1 8] directions, respectively. As the number of energetic atoms decreases due to energy transfer to the lattice, the number of amorphous atoms rises and attains a nearly constant value by 3 ps. Similar behaviour was observed for 30 keV U recoils.

The ratio of amorphous atoms to the total number of defects is an important characteristic of the primary damage state. It has important implications for defect recovery under dynamic and thermal annealing and radiation resistance. If this ratio is close to zero, the damage will consist mainly of isolated defects as in the case of silicon carbide—a highly radiation resistant ceramic [11]. This parameter has not been systematically examined in previous radiation damage simulations in

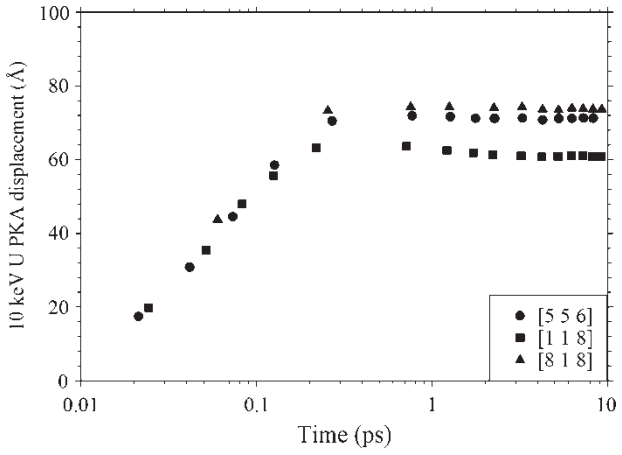

Figure 1. The displacement of 10 keV U PKAs initiated along three different crystallographic directions in zircon at 30 K as a function of time.

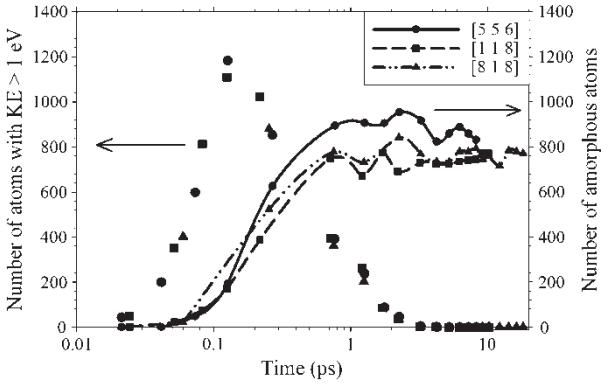

Figure 2. The number of atoms with kinetic energy in excess of 1 eV (left ordinate) and the number of amorphous atoms (right ordinate) for three 10 keV U cascades as a function of time. Lines are drawn through the data to guide the eye.

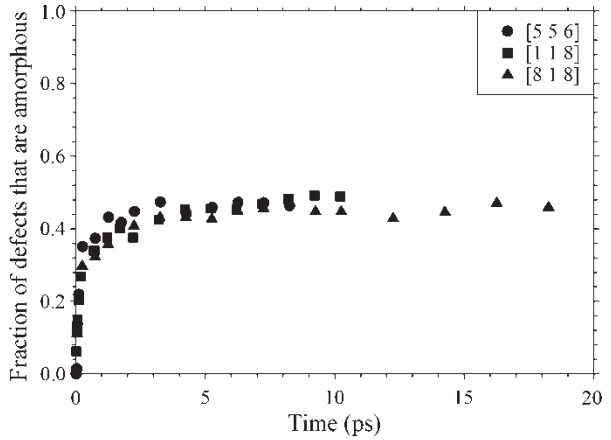

Figure 3. The evolution of the fraction of defects that are amorphous atoms in 10 keV U cascades.

ceramics. Figure 3 shows the fraction of defects created by 10 keV U recoils in $ZrSiO_4$ that are amorphous based on the criterion discussed in the previous section. Once again, the curves for the three cascades nearly coincide. A large fraction of the defects (0.46–0.50) produced in the cascade is amorphous. The total number of amorphous and defective atoms in the primary damage state are 831 and 1796 for [5 5 6], 771 and 1576 for [1 1 8] and 772 and 1681 for [8 1 8], respectively. Let us estimate the maximum possible value for the amorphous fraction in the present case. If the approximately 1600 defects produced in the cascade were all contained in a sphere with the density of zircon, the sphere would have a radius of 16 Å. Assuming that a 2 Å layer on the surface is occupied by defects and the interior is amorphous, one would obtain $(14/16)^3$ or 0.67 for the theoretical maximum amorphous fraction. The fact that the amorphous fraction is close to this value indicates that direct impact amorphisation is very effective in cascades produced by heavy recoils in zircon.

Figure 4(a) is a projection along [010] of the defects produced by a 10 keV U PKA along [5 5 6] in zircon at 30 K. In the present work, the colors green (dark gray), black and orange (light gray) are used to represent Zr, Si and O, respectively. The box shown is a small portion of the simulation cell that contains all the defects produced. The vertical axis of this box is along [001]. A dense amorphous core elongated along the direction of travel of the PKA is produced. The core can be seen in figure 4(b), which is in a similar orientation to figure 4(a), but only the amorphous atoms are represented. A small amorphous cluster is present near the main amorphous core. Unlike a typical subcascade that resembles a tree branch, this small cluster is not connected to the main amorphous core, which indicates effective energy transfer through replacement collision sequences. The difference between figure 4(a) and (b) is accounted by the defects (50–54% of the total) situated at the periphery of the amorphous core in analogy to the sphere example discussed above. For comparison, figure 5(a) and (b), respectively, show the

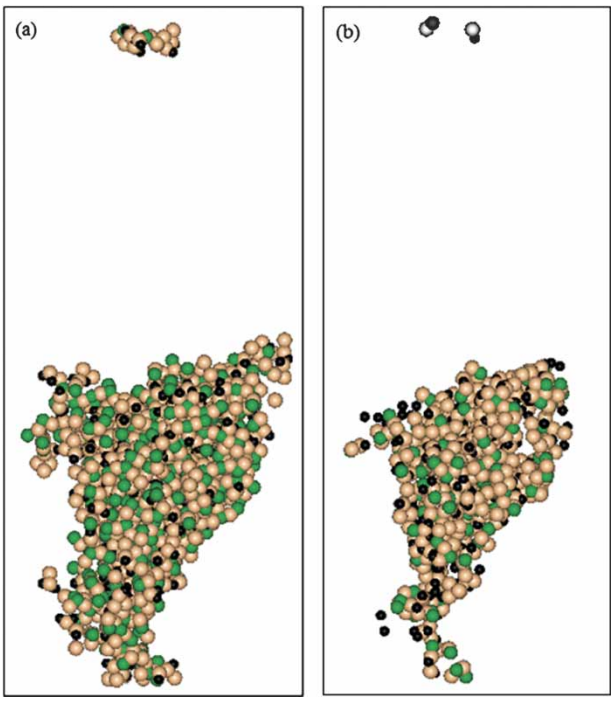

Figure 4. Orthographic projection along [010] of (a) defects and (b) amorphous atoms produced in zircon at 8.3 ps after introduction of a 10 keV U PKA at 30 K. The box shown is about 55 × 135 Å. Green (dark gray), black and orange (light gray) spheres represent Zr, Si and O atoms, respectively.

defects and amorphous core produced by a 30 keV U PKA along [5 5 6] at 30 K. At this higher energy, which is similar to the damage energy from a Th recoil in natural zircons, many more small amorphous clusters are produced that are well separated from each other and the central amorphous core. Some are enriched in Zr while others in Si relative to zircon stoichiometry. The number of amorphous atoms was 2550 (485 Zr, 599 Si and 1466 O) out of 5266 defects (1368 Zr, 1103 Si and 2795 O). This yields an amorphous fraction of 0.48 in agreement with the 10 keV PKA results. It is worth noting that the total number of defective atoms (5266) for the 30 keV damage-energy recoil is somewhat higher than the value (3800 atoms) determined by NMR for 70 keV recoils (35 keV damage energy) in natural zircons [12], but the present MD simulations do not allow nor account for the recovery and relaxation processes that are known to occur in natural zircons over geologic time scales.

In the case of the 30 keV U PKA at 300 K, the number of amorphous atoms was 2401 (474 Zr, 517 Si and 1410 O) out of 6555 defects (1603 Zr, 1052 Si and 3900 O). This yields an amorphous fraction of 0.37—much lower than the 30 K result, while one would expect a higher value at 300 K due to increased defect recombination at this higher temperature. A careful analysis of the above numbers reveals that while the number of amorphous atoms differs by about 6% between the two 30 keV cascades, the number of defects is 25% more at 300 K due to a 40% increase in O defects. Figure 6 shows isolated O defects distributed around the amorphous core and small

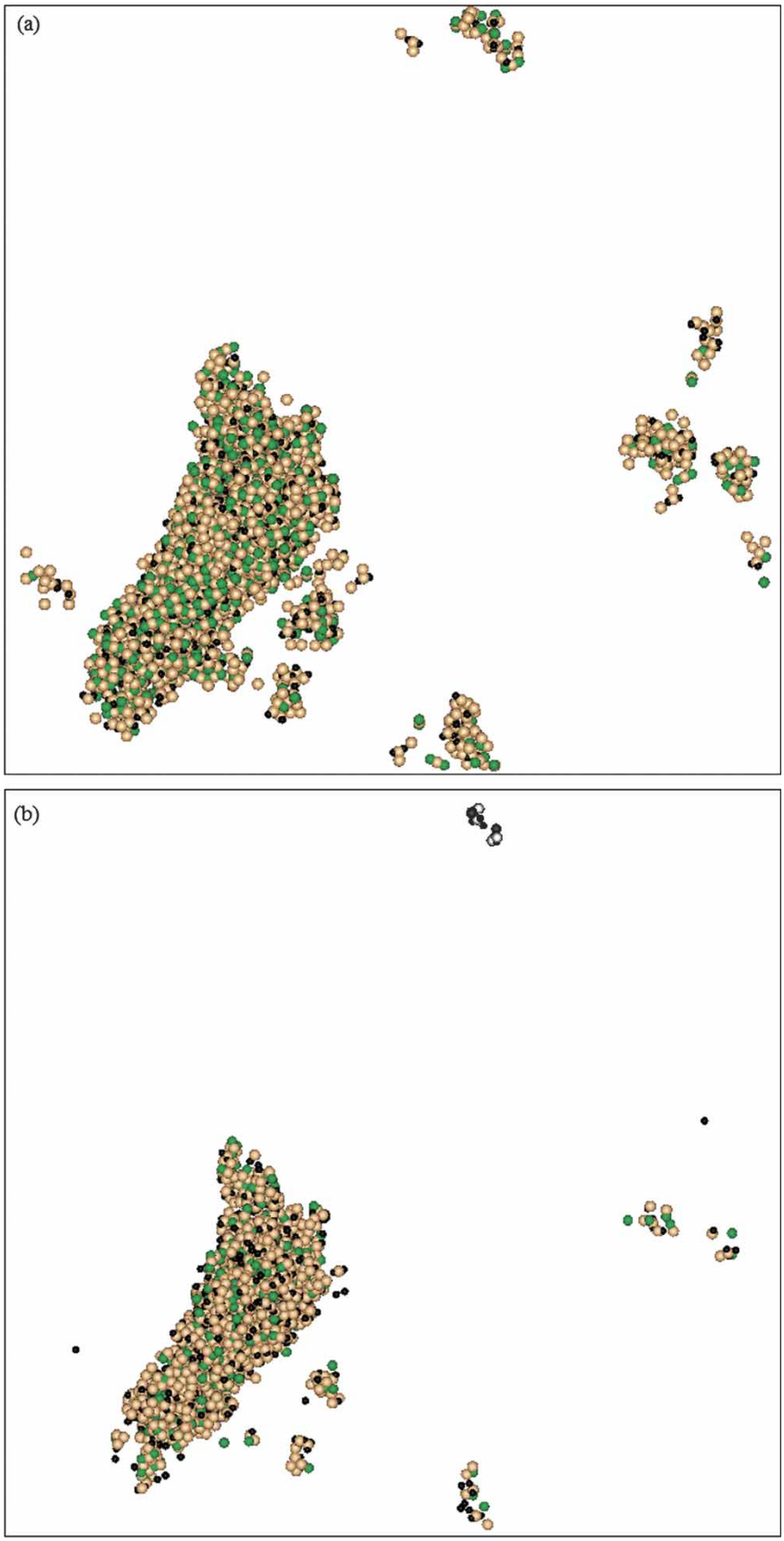

Figure 5. Orthographic projection along [010] of (a) defects and (b) amorphous atoms produced in zircon at 14.5 ps after introduction of a 30 keV U PKA at 30 K. The box shown is about 200 × 200 Å. Green (dark gray), black and orange (light gray) spheres represent Zr, Si and O atoms, respectively.

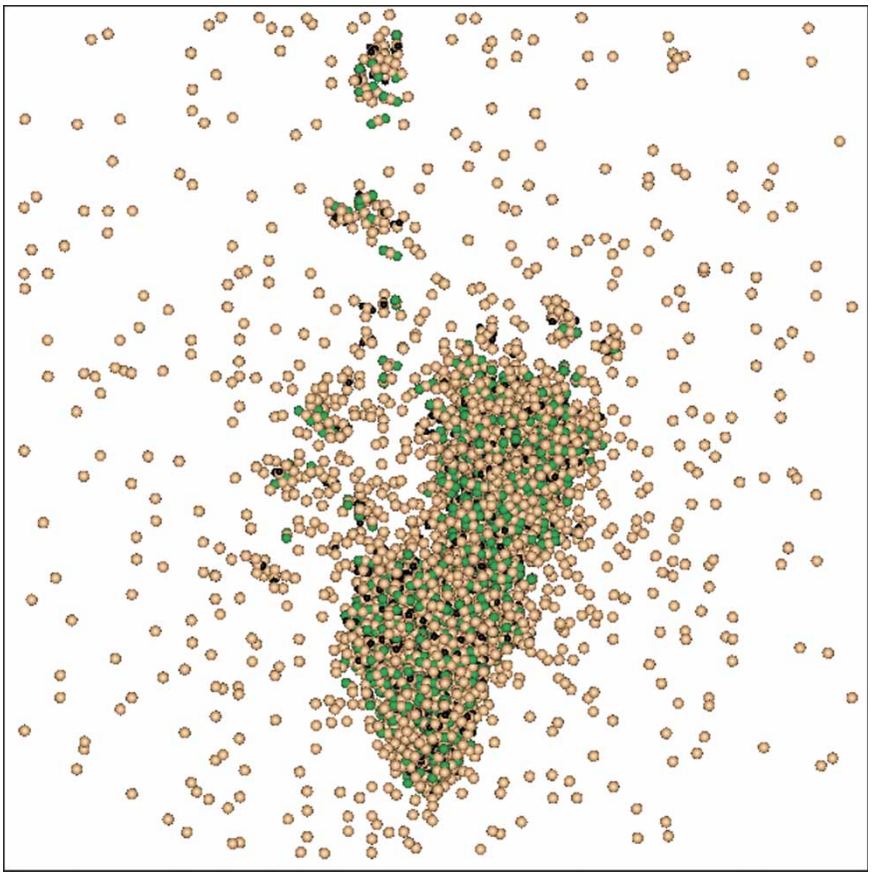

Figure 6. Orthographic projection along [010] of defects produced in zircon at 15.7 ps after introduction of a 30 keV U PKA at 300 K. The box shown is about 235 × 235 Å. Green (dark gray), black and orange (light gray) spheres represent Zr, Si and O atoms, respectively.

clusters. At the higher temperature (500 K peak temperature and 400 K final temperature), some of the Si—O bonds may stretch beyond the 2 Å cut-off used to detect O defects in the present analysis. Since this isolated O defect was not observed in the other four cascades, we believe it is due to the short cut-off used in the defect analysis. To get better insights into changes in the amorphous fraction and the distribution of amorphous clusters with PKA energy and temperature, detailed statistical studies of cascades in zircon at different temperatures and PKA energies are needed.

The present discovery of small amorphous cluster formation adds to our understanding of the primary damage state in zircon. Recently, Trachenko *et al.* [13] have discussed the percolation of disordered regions leading to amorphisation of the material. The present results show that the primary damage state in zircon can be quite complex and consist of spatially separated multiple disordered regions that differ in size and chemistry, as opposed to the traditional picture of a single amorphous core. This complexity must be taken into account in macroscopic models of damage accumulation. Moreover, at elevated temperatures, these chemically inhomogeneous clusters could play a role in nucleating nanocrystals of zirconia. The formation of randomly oriented nanocrystals of tetragonal ZrO_2 in an amorphous SiO_2 matrix has been observed during irradiation of $ZrSiO_4$ at 1050 K [14].

In an effort to understand the structural features of the primary damage the average Zr CN and the degree of Si—O—Si polymerisation were determined. The evolution of Zr defect CN for 10 keV U PKA, shown in figure 7, indicates that Zr defects are severely undercoordinated even in the ballistic phase of the cascade. The average Zr

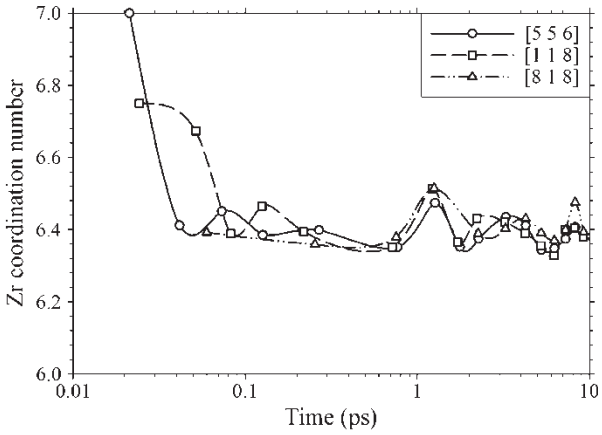

Figure 7. The average coordination number of Zr defects in three 10 keV U cascades in zircon as a function of time. Lines are drawn through the data to guide the eye.

CN attains a steady value of 6.4 after 0.2 ps with fluctuations of about ± 0.1. The final value of Zr CN was found to be 6.3 for the two 30 keV U cascades with similar fluctuations. This value is in excellent agreement with recent extended X-ray absorption fine structure experiments that show that Zr in nuclear waste glasses has a coordination number of 6.3 [15]. It is also in agreement with the value of about 7 reported by Farges and Calas [16] in amorphous zircon minerals, where some recovery or relaxation over geologic time could account for the slightly higher value of CN. The degree of polymerisation of Si, Q, is shown in figure 8 for 10 keV U PKA. Q is the average number of bridging oxygen per Si defect. In perfect crystal zircon, Si is not polymerised and so Q is zero. Q increases from about 1.2 at 0.15 ps, when amorphisation begins (see figure 2) and reaches a final value of 1.5–1.6 at about 3 ps, when the number of amorphous atoms becomes fairly constant. The final Q values were 1.5 and 1.4 for 30 keV U PKA at 30 and 300 K, respectively. This agrees with the experimental value of approximately two obtained at low doses using nuclear magnetic resonance [12]. The distribution of bridging oxygen is shown in figure 9 for 10 and 30 keV U PKA along [5 5 6] at 30 K and is nearly identical for the two cases. Thus the first neighbour environment of Zr and Si defects is quite similar for all five cascades simulated.

The bridging oxygen atoms discussed above constitute only 29–33% of O defects in 10 and 30 keV cascades simulated at 30 K. Farnan and Salje [12] have pointed out that a large number of interstitial oxygen defects need to be present in order to rationalize the polymerisation of SiO_4 tetrahedra. Figure 10 shows the evolution of bridging oxygen defects (black) and non-bridging O defects (orange/gray) that are not bonded to Si (at least 2 Å away from any Si atom). The non-bridging O defects are dominant during the ballistic phase of the cascade. As the amorphous phase starts to form (see figure 2), the number of non-bridging O defects decreases and more Si—O—Si bridges are formed. We obtain a final ratio of almost one bridging defect for two non-bridging defects in 10 and 30 keV U recoils at 30 K.

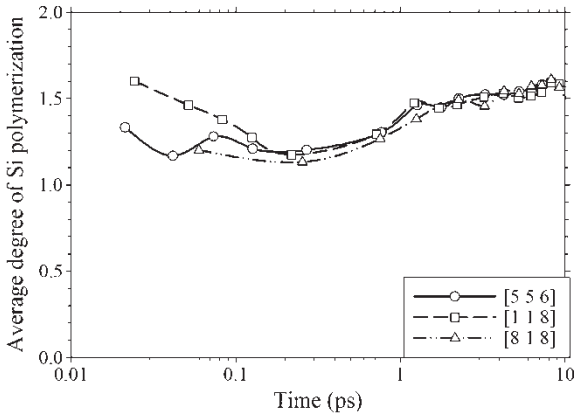

Figure 8. The average degree of polymerisation of Si defects in three 10 keV U cascades in zircon as a function of time. Lines are drawn through the data to guide the eye.

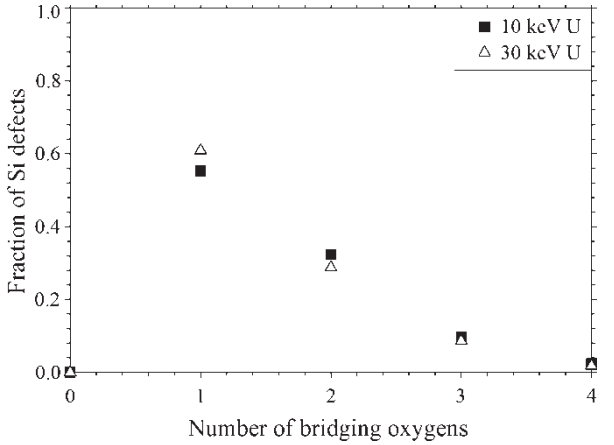

Figure 9. The distribution of the number of bridging O per Si defect for 10 and 30 keV U cascade in zircon.

In an effort to analyse the composition of the amorphous and peripheral defect regions, the relative proportions of Zr, Si, and O among defects and amorphous atoms in 10 keV U cascades were determined and are shown in figures 11 and 12, respectively. Circles, squares and triangles represent PKA along [5 5 6], [1 1 8] and [8 1 8], respectively. The data from the three cascades lie on top of each other, which shows that this is a characteristic feature of cascades in zircon. Figure 11 reveals that O defects are the most numerous and account for 52–54%, Zr defects are next at 25–26% and Si defects constitute 21–22%. The defect percentages for 30 keV U cascades are 53–60% O, 24–26% Zr and 16–21% Si defects. The proportions of Zr and Si are slightly different in the amorphous state with Si being more numerous than Zr as plotted in figure 12. Amorphous atoms are constituted by 55–57% O, 24–26% Si and 18–19% Zr. This indicates that the amorphous zones are relatively enriched in Si, while the peripheral defects are richer in Zr. As discussed by Crocombette and Ghaleb [3], such segregation across the damage zone may be a key factor in the experimentally

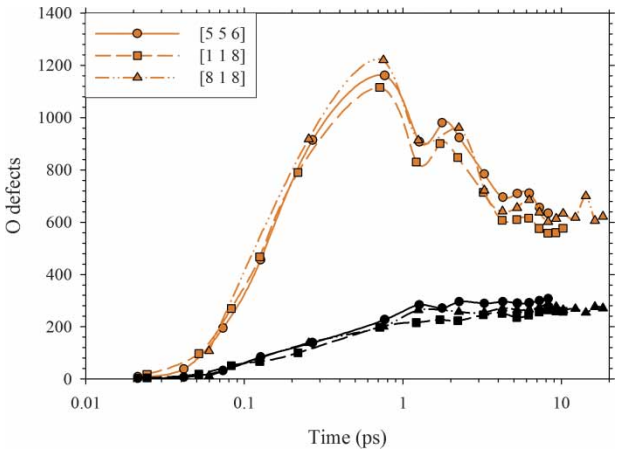

Figure 10. The number of bridging (lower black curve) and non-bridging (upper orange/gray curve) O defects as a function of time for three 10 keV U cascades in zircon. Lines are drawn through the data to guide the eye.

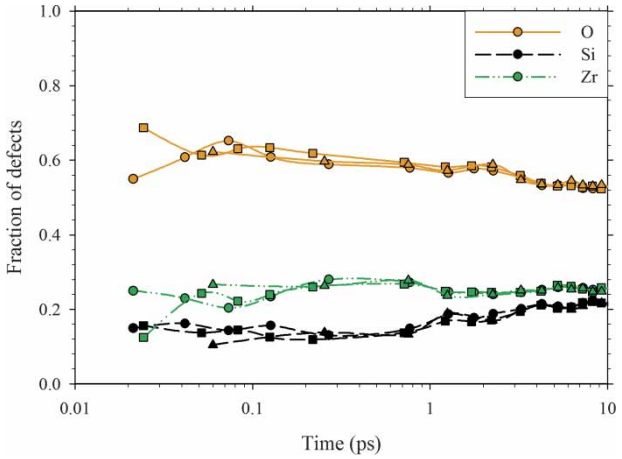

Figure 11. The relative proportions of O (solid orange/light gray line), Si (dashed black line) and Zr (dashed and dotted green/dark gray line) defects in three 10 keV U cascades in zircon as a function of time. Circles, squares and triangles represent cascades initiated along [5 5 6], [1 1 8] and [8 1 8] directions, respectively. Lines are drawn through the data to guide the eye.

observed nucleation of ZrO_2 nanocrystals in zircon irradiated at elevated temperatures [14].

The present simulations have shown that there are fundamental features that are common to heavy-ion recoil cascades in zircon regardless of PKA energy or direction. The Zr defect coordination number of about 6.3 suggests that Zr defects are surrounded by six or seven O. Si is polymerised and the average Q value is about 1.5, which is smaller than the average of 2 observed in our simulations of amorphous zircon [7]. A large volume expansion is needed to accommodate this severe Zr undercoordination and Si polymerisation, because the bond distances are not significantly changed as revealed in our previous study of disordered zircon [7]. Experimental studies ([1] and references therein) have shown that the volume expansion associated with amorphisation of zircon can be as high as 18%. Such a large volume expansion can create easy migration pathways for water and cations and enhance leaching of cations upon disordering of zircon by radiation. The observation of spatially separated amorphous clusters and non-bridging oxygen defects, extraction of insights about chemical segregation and the quantification of the amorphous fraction in the primary damage state are key contributions of the present work.

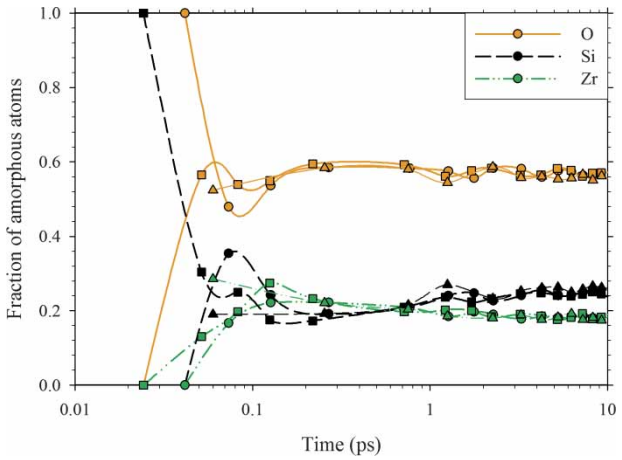

Figure 12. The relative proportions of O (solid orange/light gray line), Zr (dashed and dotted green/dark gray line), and Si (dashed black line) amorphous atoms in three 10 keV U cascades in zircon as a function of time. Circles, squares and triangles represent cascades initiated along [5 5 6], [1 1 8] and [8 1 8] directions, respectively. Lines are drawn through the data to guide the eye.

4. Conclusions

We have used MD simulations with a partial charge model and a massively parallel computer code to model 10 and 30 keV recoil damage in zircon at 30 and 300 K. The features of the cascade are direct impact amorphisation, Zr coordination number of 6.4, Si polymerisation of 1.6 bridging O per SiO_4 tetrahedron and the occurrence of twice as many non-bridging O defects as bridging O. Nearly half of the defects produced exist in the form of an amorphous core or amorphous clusters. The remaining defects are at the boundary between amorphous and crystalline regions. Chemical inhomogeneity of amorphous clusters and composition differences between the cascade core and periphery could play an important role in nanoscale segregation in zircon irradiated at elevated temperatures.

Acknowledgements

This research was supported by the Division of Materials Sciences and Engineering, Office of Basic Energy Sciences, US Department of Energy (DOE) under Contract DE-AC05-76RL01830. This research was performed in part using the Molecular Science Computing Facility in Environmental Molecular Sciences Laboratory, a national scientific user facility sponsored by the US DOE, Office of Biological and Environmental Research and located at Pacific Northwest National Laboratory. This work used resources of the National Energy Research Scientific Computing Center, which is supported by the Office of Science of the US DOE under Contract No. DE-AC03-76SF00098.

References

[1] C.S. Palenik, L. Nasdala, R.C. Ewing. Radiation damage in zircon. *Amer. Mineral.*, **88**, 770 (2003).
[2] W.J. Weber. Radiation-induced defects and amorphization in zircon. *J. Mater. Res.*, **5**, 2687 (1990).
[3] J.-P. Crocombette, D. Ghaleb. Molecular dynamics modeling of irradiation damage in pure and uranium-doped zircon. *J. Nucl. Mater.*, **295**, 167 (2001).
[4] K.O. Trachenko, M.T. Dove, E.K.H. Salje. Structural changes in zircon under α-decay irradiation. *Phys. Rev. B*, **65**, 180102 (2002).
[5] R. Devanathan, L.R. Corrales, W.J. Weber, A. Chartier, C. Meis. Molecular dynamics simulation of defect production in collision cascades in zircon. *Nucl. Instrum. Meth. B*, **228**, 299 (2005).

[6] I.T. Todorov, W. Smith, K. Trachenko, M.T. Dove. DL_POLY_3: new dimensions in molecular dynamics simulations via massive parallelism. *J. Mater. Chem.*, **16**, 1911 (2006).

[7] R. Devanathan, L.R. Corrales, W.J. Weber, A. Chartier, C. Meis. Molecular dynamics simulation of disordered zircon. *Phys. Rev. B*, **69**, 064115 (2004).

[8] J.F. Ziegler, J.P. Biersack, U. Littmark. *The Stopping and Range of Ions in Matter*, Pergamon, New York (1985).

[9] X.L. Yuan, L.W. Hobbs. Modeling chemical and topological disorder in irradiation-amorphized silicon carbide. *Nucl. Instrum. Meth. B*, **191**, 74 (2002).

[10] E. Balan, F. Mauri, C.J. Pickard, I. Farnan, G. Calas. The aperiodic states of zircon: an *ab initio* molecular dynamics study. *Amer. Mineral.*, **88**, 1769 (2003).

[11] R. Devanathan, W.J. Weber, F. Gao. Atomic scale simulation of defect production in irradiated 3C—SiC. *J. Appl. Phys.*, **90**, 2303 (2001).

[12] I. Farnan, E.K.H. Salje. The degree and nature of radiation damage in zircon observed by Si nuclear magnetic resonance. *J. Appl. Phys.*, **89**, 2084 (2001).

[13] K. Trachenko, M.T. Dove, T. Geisler, I. Todorov, W. Smith. *J. Phys. Condens. Matter*, **16**, S2623 (2004).

[14] A. Meldrum, S.J. Zinkle, L.A. Boatner, R.C. Ewing. Heavy-ion irradiation effects in the ABO_4 orthosilicates: decomposition, amorphization and recrystallization. *Phys. Rev. B*, **59**, 3981 (1999).

[15] L. Galoisy, E. Pelgrin, M.A. Arrio, P. Ildefonse, G. Calas, D. Ghaleb, C. Fillet, F. Pacaud. Evidence for 6-coordinated Zr in inactive nuclear waste glasses. *J. Amer. Ceram. Soc.*, **82**, 2219 (1999).

[16] F. Farges, G. Calas. Structural analysis of radiation damage in zircon and thorite: an X-ray absorption spectroscopic study. *Amer. Mineral.*, **76**, 60 (1991).